Wuhan University Journal of Natural Sciences

2026, Vol.31 No.5, 471-480

Article ID 1007-1202(2026)05-0471-10 DOI https://doi.org/10.1051/wujns/2026315471

Cite this article: LI Dekui, WEI Xingmin, WU Jianjun. Fixed-Time Function Combination Synchronization of the Two Chaotic System Groups with Unknown Parameters[J]. *Wuhan Univ J of Nat Sci*, 2026, 31(5): 471-480.

Fixed-Time Function Combination Synchronization of the Two Chaotic System Groups with Unknown Parameters

☐ **LI Dekui, WEI Xingmin, WU Jianjun**

School of Public Health, Gansu University of Chinese Medicine, Lanzhou 730101, Gansu, China

Abstract: In this paper, fixed-time function combination synchronization of two system groups with unknown parameters is proposed and studied, where one system group is called the drive system group made up of *n* different chaotic systems, and the other system group made up by *m* different chaotic systems is called the response system group. According to Lyapunov theorem and adaptive control technology, we devise an adaptive controller to achieve the synchronization of the two system groups. Although there are many response systems, the synchronization of the two system groups can be realized by controlling only one response system. At the same time, the designed parameter identification laws can identify accurately all the unknown parameters. The synchronization time does not rely on initial values of all the systems. Some numerical examples are given to prove the correctness of the conclusions.

Key words: function combination synchronization; unknown parameter identification; adaptive controller; fixed-time synchronization

CLC number: TP273

0 Introduction

Since Pecora and Carroll[1] have proposed the concept of chaos synchronization in 1990, infinite-time synchronization of two chaotic systems has been extensively studied[2-4], in which state variables tend to be consistent as time tends towards infinity. However, infinite-time synchronization is inconvenient in practical application because of the finiteness of machines lives. Realizing synchronization of chaotic systems is the premise and foundation of chaos application in finite time as short as possible.

In recent years, many scholars have extensively studied finite-time synchronization of chaotic systems[4-7]. The disadvantage of the finite-time synchronization is that its synchronization time completely depends on the initial values of the systems. Therefore, it is meaningful to study the fixed-time synchronization, and its synchronization time has nothing to do with the initial values of the systems. Currently, research on fixed-time synchronization has become a hot topic[8-12].

Most studies about chaotic synchronization focus on one controlled response system synchronizing with one drive system[1-12]. However, in order to obtain more complex chaotic time series to enhance the security of the secret commu-

Received date: 2025-03-17 © Wuhan University 2026

Foundation item: Supported by the National Natural Science Foundation of China (11161027) and the Gansu Province Disease Prevention and Control Scientific Research Project (GSJKKY-2025-10)

Biography: LI Dekui, male, Professor, research direction: theory and apply of chaotic system. E-mail: dkli2009@163.com

This is an Open Access article distributed under the terms of the Creative Commons Attribution License (https://creativecommons.org/ licenses/by/4.0), which permits unrestricted use, distribution, and reproduction in any medium, provided the original work is properly cited.

nication, combination synchronization has been studied. Wang *et al*[13] have achieved the combination synchronization of two drive systems and one response system. Compound-combination synchronization of five chaotic systems has been studied which are three drive systems and two response ones[14]. The function combination synchronization of three identical chaotic systems has been realized by an appropriate control law[15]. The generalized function projective combination synchronization is studied based on the tracking control technique, where the scaling functions are nonlinear and the active control method cannot be used in this scheme since its error is large[16]. The adaptive function projective combination synchronization of three fractional-order chaotic systems is realized based on the stability theory of fractional-order systems and tracking control[17]. Zheng[18] has studied the multi-switching combination synchronization of three different chaotic systems.

Almost all the combination synchronization of chaotic systems involves a small number of the drive systems or the response ones. Only in Ref. [19], the combination synchronization of four drive systems and four response systems is realized. In short, the number of the drive systems and the response ones is small in the existing studies on combination synchronization, so it is very necessary to study the combination synchronization of any number of chaotic systems.

Motivated by the above discussion, we study the fixed-time function combination synchronization of n drive systems and m response systems. All the systems contain unknown parameters which need to be identified in the process of realizing combination synchronization. This synchronization of the drive system group and the response system group is extremely complex. Therefore, the transmitted information will be more secure and reliable when this synchronization method of chaotic systems is used to implement secure communication.

1 Models of Two System Groups and Preliminaries

Function combination synchronization of the drive system group with n systems and response system group with m systems will be presented. It is worth mentioning that $n \in \mathbb{Z}_+$ can be equal or unequal with $m \in \mathbb{Z}_+$. The drive system group with unknown parameters is shown as follows,

$$\dot{\boldsymbol{x}}_1 = \boldsymbol{C}_1(\boldsymbol{x}_1)\boldsymbol{A}_1 + \boldsymbol{f}_1(\boldsymbol{x}_1),\ \dot{\boldsymbol{x}}_2 = \boldsymbol{C}_2(\boldsymbol{x}_2)\boldsymbol{A}_2 + \boldsymbol{f}_2(\boldsymbol{x}_2),\ \cdots,\ \dot{\boldsymbol{x}}_n = \boldsymbol{C}_n(\boldsymbol{x}_n)\boldsymbol{A}_n + \boldsymbol{f}_n(\boldsymbol{x}_n), \tag{1}$$

where $\boldsymbol{A}_i = (a_{i1}, a_{i2}, \cdots, a_{ik})^{\mathrm{T}} \in \mathbb{R}^k$ and $\boldsymbol{x}_i(t) = (x_{i1}, x_{i2}, \cdots, x_{ik})^{\mathrm{T}} \in \mathbb{R}^k$ are the unknown parameter vector and the state variable vector of the i-th drive system, respectively, $\boldsymbol{C}_i(\boldsymbol{x}_i)\boldsymbol{A}_i$ and $\boldsymbol{f}_i(\boldsymbol{x}_i)$ are linear and nonlinear parts of the i-th drive system, respectively, where $i = 1, 2, \cdots, n$. At the same time, the response system group with m chaotic systems is shown as follows,

$$\dot{\boldsymbol{y}}_1 = \boldsymbol{D}_1(\boldsymbol{y}_1)\boldsymbol{B}_1 + \boldsymbol{g}_1(\boldsymbol{y}_1),\ \dot{\boldsymbol{y}}_2 = \boldsymbol{D}_2(\boldsymbol{y}_2)\boldsymbol{B}_2 + \boldsymbol{g}_2(\boldsymbol{y}_2),\ \cdots,\ \dot{\boldsymbol{y}}_m = \boldsymbol{D}_m(\boldsymbol{y}_m)\boldsymbol{B}_m + \boldsymbol{g}_m(\boldsymbol{y}_m), \tag{2}$$

where $\boldsymbol{y}_j = (y_{j1}, y_{j2}, \cdots, y_{jk})^{\mathrm{T}} \in \mathbb{R}^k$ and $\boldsymbol{B}_j = (b_{j1}, b_{j2}, \cdots, b_{jk})^{\mathrm{T}} \in \mathbb{R}^k$ are the state variable vector and the uncertain parameter vector of the j-th response system respectively, $\boldsymbol{D}_j(\boldsymbol{y}_j)\boldsymbol{B}_j$ and $\boldsymbol{g}_j(\boldsymbol{y}_j)$ are linear and nonlinear parts of the j-th response system respectively, $j = 1, 2, \cdots, m$. $\boldsymbol{u}_s = (u_{s1}, u_{s2}, \cdots, u_{sk})^{\mathrm{T}} \in \mathbb{R}^k$ is the synchronization controller added on the s-th response system. The range of subscript s ($s = 1, 2, 3, \cdots, m$) means that realizing synchronization only needs control any one of the response systems, so it is very flexible to control the response system.

Definition 1 Let $\boldsymbol{\alpha}_i(t) = \mathrm{diag}(\alpha_{i1}(t), \alpha_{i2}(t), \cdots, \alpha_{ik}(t))$ and $\boldsymbol{\beta}_j(t) = \mathrm{diag}(\beta_{j1}(t), \beta_{j2}(t), \cdots, \beta_{jk}(t))$ ($i = 1, 2, \cdots, n, j = 1, 2, \cdots, m$) are $m+n$ arbitrary nonzero diagonal function matrices. If the drive system group (1) and the response system group (2) can satisfy

$$\boldsymbol{\Omega} = \{(\boldsymbol{x}_i, \boldsymbol{y}_j) \mid \sum_{i=1}^{n} \boldsymbol{\alpha}_i(t)\boldsymbol{x}_i = \sum_{j=1}^{m} \boldsymbol{\beta}_j(t)\boldsymbol{y}_j\}, \tag{3}$$

then function combination synchronization of the drive system group (1) and the response system group (2) is achieved.

In terms of the forms and the number of the scaling function matrices and the systems involved, it is easy to find that the function combination synchronization studied in this paper is a generalization of the existing synchronization models, and the models mentioned above can be regarded as its special cases, such as dual synchronization, combination synchronization and function projective synchronization.

Based on Definition 1, the function combination synchronization error of the drive system group (1) and the response system group (2) is shown as follows,

$$\boldsymbol{e} = \sum_{j=1}^{m} \boldsymbol{\beta}_j(t)\boldsymbol{y}_j - \sum_{i=1}^{n} \boldsymbol{\alpha}_i(t)\boldsymbol{x}_i. \tag{4}$$

Definition 2 If the error (4) can tend to zero within the time T, then the drive system group (1) and the response system group (2) realize the fixed-time function combination synchronization, where T is a positive constant independent of the initial values of the systems.

We constructed an adaptive controller and identification laws of the unknown parameters to realize the fixed-time function combination synchronization of the drive system group (1) and the response system group (2). To this end, the following lemmas are needed.

Lemma 1[20] Let $V(t)$ be a positive and differentiable function, if the inequality

$$\dot{V}(t)\leqslant -\lambda V^{\varepsilon}(t)-\mu V^{\delta}(t) \tag{5}$$

holds for any real numbers $\lambda>0$, $\mu>0$, $0<\varepsilon<1$, $\delta>1$. $V(t)\equiv 0$ as $t\geqslant T$, then

$$T\leqslant \frac{1}{\lambda}\left(\frac{\lambda}{\mu}\right)^{\frac{1-\varepsilon}{\delta-\varepsilon}}\left(\frac{1}{1-\varepsilon}+\frac{1}{\delta-1}\right). \tag{6}$$

Lemma 2[20] For any real numbers $\alpha_i\,(i=1,2,3,\cdots,n)$, $0<r<1$ and $k>1$, the following two inequalities hold.

$$\left(\sum_{i=1}^{n}|\alpha_i|\right)^{r}\leqslant \sum_{i=1}^{n}|\alpha_i|^{r},\ n\left(\frac{1}{n}\sum_{i=1}^{n}|\alpha_i|\right)^{k}\leqslant \sum_{i=1}^{n}|\alpha_i|^{k}. \tag{7}$$

2 The Fixed-Time Function Combination Synchronization

According to (1)-(4), the error system of two system groups is shown as follows,

$$\begin{aligned}\dot{\boldsymbol{e}}&=\sum_{j=1}^{m}\dot{\boldsymbol{\beta}}_j(t)\boldsymbol{y}_j+\sum_{j=1}^{m}\boldsymbol{\beta}_j(t)\dot{\boldsymbol{y}}_j-\sum_{i=1}^{n}\dot{\boldsymbol{\alpha}}_i(t)\boldsymbol{x}_i-\sum_{i=1}^{n}\boldsymbol{\alpha}_i(t)\dot{\boldsymbol{x}}_i\\&=\sum_{j=1}^{m}\dot{\boldsymbol{\beta}}_j(t)\boldsymbol{y}_j+\sum_{j=1}^{m}\boldsymbol{\beta}_j(t)\boldsymbol{D}_j(\boldsymbol{y}_j)\boldsymbol{B}_j+\sum_{j=1}^{m}\boldsymbol{\beta}_j(t)\boldsymbol{g}_j(\boldsymbol{y}_j)-\sum_{i=1}^{n}\dot{\boldsymbol{\alpha}}_i(t)\boldsymbol{x}_i-\sum_{i=1}^{n}\boldsymbol{\alpha}_i(t)\boldsymbol{C}_i(\boldsymbol{x}_i)\boldsymbol{A}_i-\sum_{i=1}^{n}\boldsymbol{\alpha}_i(t)\boldsymbol{f}_i(\boldsymbol{x}_i)+\boldsymbol{\beta}_s(t)\boldsymbol{u}_s.\end{aligned} \tag{8}$$

Theorem 1 If the adaptive controller and the parameter identification laws are constructed as follows,

$$\begin{aligned}\boldsymbol{u}_s=\frac{1}{\boldsymbol{\beta}_s(t)}[&-\sum_{j=1}^{m}\dot{\boldsymbol{\beta}}_j(t)\boldsymbol{y}_j-\sum_{j=1}^{m}\boldsymbol{\beta}_j(t)\boldsymbol{D}_j(\boldsymbol{y}_j)\tilde{\boldsymbol{B}}_j-\sum_{j=1}^{m}\boldsymbol{\beta}_j(t)\boldsymbol{g}_j(\boldsymbol{y}_j)+\sum_{i=1}^{n}\dot{\boldsymbol{\alpha}}_i(t)\boldsymbol{x}_i\\&+\sum_{i=1}^{n}\boldsymbol{\alpha}_i(t)\boldsymbol{C}_i(\boldsymbol{x}_i)\tilde{\boldsymbol{A}}_i+\sum_{i=1}^{n}\boldsymbol{\alpha}_i(t)\boldsymbol{f}_i(\boldsymbol{x}_i)-\operatorname{sign}(\boldsymbol{e})|\boldsymbol{e}|^{\alpha}-\operatorname{sign}(\boldsymbol{e})|\boldsymbol{e}|^{\beta}],\end{aligned} \tag{9}$$

$$\begin{cases}\dot{\tilde{\boldsymbol{A}}}_i=-\boldsymbol{e}^{\mathrm{T}}\boldsymbol{\alpha}_i(t)\boldsymbol{C}_i(\boldsymbol{x}_i)+\operatorname{sign}(\hat{\boldsymbol{A}}_i)\|\hat{\boldsymbol{A}}_i\|^{\alpha}+\operatorname{sign}(\hat{\boldsymbol{A}}_i)\|\hat{\boldsymbol{A}}_i\|^{\beta},\\ \dot{\tilde{\boldsymbol{B}}}_j=\boldsymbol{e}^{\mathrm{T}}\boldsymbol{\beta}_j(t)\boldsymbol{D}_j(\boldsymbol{y}_j)+\operatorname{sign}(\hat{\boldsymbol{B}}_j)\|\hat{\boldsymbol{B}}_j\|^{\alpha}+\operatorname{sign}(\hat{\boldsymbol{B}}_j)\|\hat{\boldsymbol{B}}_j\|^{\beta},\end{cases} \tag{10}$$

then the fixed-time function combination synchronization of the system groups (1) and (2) can be achieved, where $\tilde{\boldsymbol{A}}_i$ and $\tilde{\boldsymbol{B}}_j$ are the estimations of $\boldsymbol{A}_i$ and $\boldsymbol{B}_j$ respectively, $0<\alpha<1$, $\beta>1$, $\hat{\boldsymbol{A}}_i=\boldsymbol{A}_i-\tilde{\boldsymbol{A}}_i$ and $\hat{\boldsymbol{B}}_j=\boldsymbol{B}_j-\tilde{\boldsymbol{B}}_j$.

Proof Substituting (9) into (8), the error system (8) is converted into

$$\dot{\boldsymbol{e}}=\sum_{j=1}^{m}\boldsymbol{\beta}_j(t)\boldsymbol{D}_j(\boldsymbol{y}_j)\hat{\boldsymbol{B}}_j-\sum_{i=1}^{n}\boldsymbol{\alpha}_i(t)\boldsymbol{C}_i(\boldsymbol{x}_i)\hat{\boldsymbol{A}}_i-\operatorname{sign}(\boldsymbol{e})|\boldsymbol{e}|^{\alpha}-\operatorname{sign}(\boldsymbol{e})|\boldsymbol{e}|^{\beta}. \tag{11}$$

We construct a Lyapunov function as follows,

$$V(t)=\frac{1}{2}\boldsymbol{e}^{\mathrm{T}}\boldsymbol{e}+\frac{1}{2}\sum_{i=1}^{n}\hat{\boldsymbol{A}}_i^{\mathrm{T}}\hat{\boldsymbol{A}}_i+\frac{1}{2}\sum_{j=1}^{m}\hat{\boldsymbol{B}}_j^{\mathrm{T}}\hat{\boldsymbol{B}}_j, \tag{12}$$

$V(t)\geqslant 0$ is obvious, then we can get

$$\begin{aligned}\dot{V}(t)&=\boldsymbol{e}^{\mathrm{T}}\dot{\boldsymbol{e}}-\sum_{i=1}^{n}\hat{\boldsymbol{A}}_i^{\mathrm{T}}\dot{\tilde{\boldsymbol{A}}}_i-\sum_{j=1}^{m}\hat{\boldsymbol{B}}_j^{\mathrm{T}}\dot{\tilde{\boldsymbol{B}}}_j\\&=\boldsymbol{e}^{\mathrm{T}}\sum_{j=1}^{m}\boldsymbol{\beta}_j(t)\boldsymbol{D}_j(\boldsymbol{y}_j)\hat{\boldsymbol{B}}_j-\boldsymbol{e}^{\mathrm{T}}\sum_{i=1}^{n}\boldsymbol{\alpha}_i(t)\boldsymbol{C}_i(\boldsymbol{x}_i)\hat{\boldsymbol{A}}_i-\boldsymbol{e}^{\mathrm{T}}\operatorname{sign}(\boldsymbol{e})|\boldsymbol{e}|^{\alpha}-\boldsymbol{e}^{\mathrm{T}}\operatorname{sign}(\boldsymbol{e})|\boldsymbol{e}|^{\beta}-\sum_{i=1}^{n}\hat{\boldsymbol{A}}_i^{\mathrm{T}}\dot{\tilde{\boldsymbol{A}}}_i-\sum_{j=1}^{m}\hat{\boldsymbol{B}}_j^{\mathrm{T}}\dot{\tilde{\boldsymbol{B}}}_j.\end{aligned} \tag{13}$$

Substituting (10) into (13), we can get

$$\dot{V}(t)=-[\boldsymbol{e}^{\mathrm{T}}\operatorname{sign}(\boldsymbol{e})|\boldsymbol{e}|^{\alpha}+\sum_{i=1}^{n}\hat{\boldsymbol{A}}_i^{\mathrm{T}}\operatorname{sign}(\hat{\boldsymbol{A}}_i)\|\hat{\boldsymbol{A}}_i\|^{\alpha}+\sum_{j=1}^{m}\hat{\boldsymbol{B}}_j^{\mathrm{T}}\operatorname{sign}(\hat{\boldsymbol{B}}_j)\|\hat{\boldsymbol{B}}_j\|^{\alpha}]$$

$$-[\mathrm{sign}(\boldsymbol{e})|\boldsymbol{e}|^{\beta}+\sum_{i=1}^{n}\hat{\boldsymbol{A}}_i{}^{\mathrm{T}}\mathrm{sign}(\hat{\boldsymbol{A}}_i)\left\|\hat{\boldsymbol{A}}_i\right\|^{\beta}+\sum_{j=1}^{m}\hat{\boldsymbol{B}}_j{}^{\mathrm{T}}\mathrm{sign}(\hat{\boldsymbol{B}}_j)\left\|\hat{\boldsymbol{B}}_j\right\|^{\beta}]$$

$$=-2^{\frac{1+\alpha}{2}}[\sum_{p=1}^{k}(\frac{e_i^2}{2})^{\frac{1+\alpha}{2}}+\sum_{i=1}^{n}\sum_{q=1}^{k}(\frac{\hat{a}_{iq}^2}{2})^{\frac{1+\alpha}{2}}+\sum_{j=1}^{m}\sum_{r=1}^{k}(\frac{\hat{b}_{jr}^2}{2})^{\frac{1+\alpha}{2}}]-2^{\frac{1+\beta}{2}}[\sum_{p=1}^{k}(\frac{e_i^2}{2})^{\frac{1+\beta}{2}}+\sum_{i=1}^{n}\sum_{q=1}^{k}(\frac{\hat{a}_{iq}^2}{2})^{\frac{1+\beta}{2}}+\sum_{j=1}^{m}\sum_{r=1}^{k}(\frac{\hat{b}_{jr}^2}{2})^{\frac{1+\beta}{2}}]. \quad (14)$$

Based on Lemma 2, we can get

$$\dot{V}(t)<-2^{\frac{1+\alpha}{2}}(\sum_{p=1}^{k}\frac{e_i^2}{2}+\sum_{i=1}^{n}\sum_{q=1}^{k}\frac{\hat{a}_{iq}^2}{2}+\sum_{j=1}^{m}\sum_{i=1}^{k}\frac{\hat{b}_i^2}{2})^{\frac{1+\alpha}{2}}-2^{\frac{1+\beta}{2}}[k(n+m+1)]^{\frac{1-\beta}{2}}(\sum_{i=1}^{k}\frac{e_i^2}{2}+\sum_{i=1}^{n}\sum_{q=1}^{k}\frac{\hat{a}_{iq}^2}{2}+\sum_{j=1}^{m}\sum_{r=1}^{k}\frac{\hat{b}_{jr}^2}{2})^{\frac{1+\beta}{2}}$$

$$=-2^{\frac{1+\alpha}{2}}[\frac{1}{2}\boldsymbol{e}^{\mathrm{T}}\boldsymbol{e}+\frac{1}{2}\sum_{i=1}^{n}\hat{\boldsymbol{A}}_i^{\mathrm{T}}\hat{\boldsymbol{A}}_i+\frac{1}{2}\sum_{j=1}^{m}\hat{\boldsymbol{B}}_j^{\mathrm{T}}\hat{\boldsymbol{B}}_j]^{\frac{1+\alpha}{2}}-2^{\frac{1+\beta}{2}}[k(n+m+1)]^{\frac{1-\beta}{2}}[\frac{1}{2}\boldsymbol{e}^{\mathrm{T}}(t)\boldsymbol{e}(t)+\frac{1}{2}\sum_{i=1}^{n}\hat{\boldsymbol{A}}_i^{\mathrm{T}}\hat{\boldsymbol{A}}_i+\frac{1}{2}\sum_{j=1}^{m}\hat{\boldsymbol{B}}_j^{\mathrm{T}}\hat{\boldsymbol{B}}_j]^{\frac{1+\beta}{2}}$$

$$=-2^{\frac{1+\alpha}{2}}[V(t)]^{\frac{1+\alpha}{2}}-2^{\frac{1+\beta}{2}}[k(n+m+1)]^{\frac{1-\beta}{2}}[V(t)]^{\frac{1+\beta}{2}}\leqslant 0. \quad (15)$$

Based on Lyapunov stability theorem and Lemma 1, there exists $T>0$ such that $\boldsymbol{e}(t)=0$ as $t\geqslant T$, which means that the fixed-time function combination synchronization of the two system groups (1) and (2) is realized in time T.

3 Synchronization Time Analysis

Based on Lemma 1 and (15), we can get

$$\lambda=2^{\frac{1+\alpha}{2}},\ \mu=2^{\frac{1+\beta}{2}}[k(n+m+1)]^{\frac{1-\beta}{2}},\ \varepsilon=\frac{1+\alpha}{2},\ \delta=\frac{1+\beta}{2}. \quad (16)$$

Substituting (16) into (6), the settling time T is obtained as follows,

$$T\leqslant\frac{1}{\lambda}(\frac{\lambda}{\mu})^{\frac{1-\varepsilon}{\delta-\varepsilon}}(\frac{1}{1-\varepsilon}+\frac{1}{\delta-1})=2^{-\frac{1+\alpha}{2}}[2^{\frac{\alpha-\beta}{2}}(kn+km+k)^{\frac{\beta-1}{2}}]^{\frac{1-\alpha}{\beta-\alpha}}(\frac{2}{1-\alpha}+\frac{2}{\beta-1}). \quad (17)$$

Generally, when systems of the drive system group and the response system group are selected in practical problems, the number of systems (n and m) and system dimension (k) will be known values, so the synchronization time is determined by α and β in the fixed-time synchronization.

According to (17), we construct a binary function of α and β to analyse the synchronization time as follows,

$$g(\alpha,\beta)=2^{-\frac{1+\alpha}{2}}(2^{\frac{\alpha-\beta}{2}}(kn+km+k)^{\frac{\beta-1}{2}})^{\frac{1-\alpha}{\beta-\alpha}}(\frac{2}{1-\alpha}+\frac{2}{\beta-1})=\frac{\alpha-\beta}{(\alpha-1)(\beta-1)}(kn+km+k)^{\frac{(\alpha-1)(\beta-1)}{2(\alpha-\beta)}}, \quad (18)$$

where $0<\alpha<1$ and $\beta>1$. The two partial derivatives of $g(\alpha,\beta)$ with respect to α and β are calculated as follows,

$$\begin{cases}g'_{\alpha}=(kn+km+k)^{\frac{(\beta-1)(\alpha-1)}{2(\alpha-\beta)}}[\dfrac{1}{(\alpha-1)^2}-\dfrac{(\beta-1)\ln\sqrt{kn+km+k}}{(\alpha-\beta)(\alpha-1)}],\\ g'_{\beta}=(kn+km+k)^{\frac{(\beta-1)(\alpha-1)}{2(\alpha-\beta)}}[\dfrac{(\alpha-1)\ln\sqrt{kn+km+k}}{(\alpha-\beta)(\beta-1)}-\dfrac{1}{(\beta-1)^2}].\end{cases} \quad (19)$$

Let $g'_{\alpha}=0$ and $g'_{\beta}=0$. We can get

$$\begin{cases}\alpha=1-\dfrac{\beta-1}{(\beta-1)\ln\sqrt{kn+km+k}-1},\\ \beta=1+\dfrac{\alpha-1}{(\alpha-1)\ln\sqrt{kn+km+k}+1}.\end{cases} \quad (20)$$

It can be seen that the two relations in (20) are implicit. Since α and β can take arbitrary values within their respective ranges $\alpha\in(0,1)$ and $\beta\in(1,+\infty)$, the function $g(\alpha,\beta)$ has no minimum point. At the same time, when $0<\alpha<1$, $\beta>1+\dfrac{1}{\ln\sqrt{kn+km+k}}$; when $\beta>1$, $0<\alpha<1-\dfrac{1}{\ln\sqrt{kn+km+k}}$; that is to say that the value range of α and β is not contradictory.

4 Numerical Simulations

In this section, five typical chaotic systems are selected to analyze the synchronization time and verify the effectiveness of the proposed adaptive controller and parameter update laws. Three of them constitute the drive system

group, and the other two constitute the response system group.

4.1 Two System Groups

We select the Lorenz system, the Chen system and the Lü system to compose the drive system group. Lorenz system[21] is

$$\dot{x}_{11}=a_1(x_{12}-x_{11}),\ \dot{x}_{12}=a_2x_{11}-x_{11}x_{13}-x_{12},\ \dot{x}_{13}=x_{11}x_{12}+a_3x_{13}, \tag{21}$$

where a_1, a_2, a_3 are unknown parameters, their true values are taken as $a_1=10$, $a_2=28$ and $a_3=-8/3$. With these parameter values, the Lorenz system exhibits chaotic behavior. Chen system[21] is

$$\dot{x}_{21}=b_1(x_{22}-x_{21}),\ \dot{x}_{22}=-7x_{21}-x_{21}x_{23}+b_2x_{22},\ \dot{x}_{23}=x_{21}x_{22}-b_3x_{23}, \tag{22}$$

where b_1, b_2, b_3 are unknown parameters, their true values are taken as $b_1=35$, $b_2=28$ and $b_3=3$. With these parameter values, the Chen system exhibits chaotic behavior. Lü system[21] is

$$\dot{x}_{31}=c_1(x_{32}-x_{31}),\ \dot{x}_{32}=-x_{31}x_{33}+c_2x_{32},\ \dot{x}_{33}=x_{31}x_{32}-c_3x_{33}, \tag{23}$$

where c_1, c_2, c_3 are unknown parameters, their true values are taken as $c_1=36$, $c_2=20$ and $c_3=3$. With these parameter values, the Lü system exhibits chaotic behavior.

Comparing (21), (22) and (23) with the drive system group (1), we can get

$$\boldsymbol{C}_1(\boldsymbol{x}_1)=\mathrm{diag}\left(x_{12}-x_{11},x_{11},x_{13}\right),\ \boldsymbol{A}_1=\left(a_1,a_2,a_3\right)^{\mathrm{T}},\ \boldsymbol{f}_1(\boldsymbol{x}_1)=\left(0,-x_{11}x_{13}-x_{12},x_{11}x_{12}\right)^{\mathrm{T}}, \tag{24}$$

$$\boldsymbol{C}_2(\boldsymbol{x}_2)=\mathrm{diag}\left(\mathrm{x}_{22}-x_{21},x_{22},-x_{23}\right),\ \boldsymbol{A}_2=\left(b_1,b_2,b_3\right)^{\mathrm{T}},\ \boldsymbol{f}_2(\boldsymbol{x}_2)=\left(0,-7x_{21}-x_{21}x_{23},\ x_{21}x_{22}\right)^{\mathrm{T}}, \tag{25}$$

$$\boldsymbol{C}_3(\boldsymbol{x}_3)=\mathrm{diag}\left(x_{32}-x_{31},x_{32},-x_{33}\right),\ \boldsymbol{A}_3=\left(c_1,c_2,c_3\right),\ \boldsymbol{f}_3(\boldsymbol{x}_3)=\left(0,-x_{31}x_{33},\ x_{31}x_{32}\right), \tag{26}$$

where $\boldsymbol{x}_1=\left(x_{11},x_{12},x_{13}\right)^{\mathrm{T}}$, $\boldsymbol{x}_2=\left(x_{21},x_{22},x_{23}\right)^{\mathrm{T}}$, $\boldsymbol{x}_3=\left(x_{31},x_{32},x_{33}\right)^{\mathrm{T}}$.

We select the Rössler system[22] and the Lorenz-like system[23] as the response system group, the Rössler system is described as follows,

$$\dot{y}_{11}=d_1(y_{12}+y_{13}),\ \dot{y}_{12}=y_{11}+d_2y_{12},\ \dot{y}_{13}=0.2+d_3y_{13}+y_{11}y_{13}, \tag{27}$$

where d_1, d_2, d_3 are unknown parameters, their true values are taken as $d_1=-1$, $d_2=0.2$ and $d_3=-5$. With these parameter values, the Rössler system exhibits periodic behavior. The Lorenz-like system is described as follows,

$$\dot{y}_{21}=f_1(y_{22}-y_{21}),\ \dot{y}_{22}=f_2y_{21}-y_{21}y_{23},\ \dot{y}_{23}=4y_{21}^2-f_3y_{23}, \tag{28}$$

where f_1, f_2, f_3 are unknown parameters, their true values are taken as $f_1=10, f_2=40, f_3=2.5$. With these parameter values, the Lorenz-like system exhibits chaotic behavior.

Comparing (27) and (28) with the response system group (2), we can get

$$\boldsymbol{D}_1(\boldsymbol{y}_1)=\mathrm{diag}\left(y_{12}+y_{13},y_{12},y_{13}\right),\ \boldsymbol{B}_1=\left(d_1,d_2,d_3\right)^{\mathrm{T}},\ \boldsymbol{g}_1(\boldsymbol{y}_1)=\left(0,y_{11},0.2+y_{11}y_{13}\right)^{\mathrm{T}}, \tag{29}$$

$$\boldsymbol{D}_2(\boldsymbol{y}_2)=\mathrm{diag}\left(y_{22}-y_{21},y_{21},-y_{23}\right),\ \boldsymbol{B}_2=\left(f_1,f_2,f_3\right)^{\mathrm{T}},\ \boldsymbol{g}_2(\boldsymbol{y}_2)=\left(0,-y_{21}y_{23},4y_{21}^2\right)^{\mathrm{T}}, \tag{30}$$

where $\boldsymbol{y}_1=\left(y_{11},y_{12},y_{13}\right)^{\mathrm{T}}$, $\boldsymbol{y}_2=\left(y_{21},y_{22},y_{23}\right)^{\mathrm{T}}$.

4.2 Calculation of Synchronization Time

From (17) and (18), we know synchronization time of the fixed-time function combination synchronization of the drive system group (1) and the response system group (2) satisfies $T\leqslant g(\alpha,\beta)$. Generally, humans always hope that synchronization time is as short as possible, but we have not found the minimum value of the binary function $g(\alpha,\beta)$. In numerical simulation, $g(\alpha,\beta)$ can be rewritten as follows,

$$g(\alpha,\beta)=\frac{\alpha-\beta}{(\alpha-1)(\beta-1)}\left(\sqrt{18}\right)^{\frac{(\alpha-1)(\beta-1)}{(\alpha-\beta)}}. \tag{31}$$

According to the scope requirements of α and β, we find the minimum of the function $g(\alpha,\beta)$ on the plane ($\alpha=0.001{:}0.001{:}0.999$ and $\beta=1.001{:}0.001{:}10$) by using computer program. Finally, we find the minimum of the function $g(\alpha,\beta)$ is 3.928 423, and the minimum point is $(\alpha,\beta)=(0.247, 9.535)$. In other words, if we select $\alpha=0.247$ and $\beta=9.535$, the drive system group (21)-(23) and the response system group (27)-(28) can realize the function combination synchronization within 3.928 423 s.

4.3 Inspection of the Controller and the Parameter Identification Laws

We select arbitrarily the scaling function matrices as follows,

$$\begin{cases}\boldsymbol{\alpha}_1=\mathrm{diag}(4+\sin t,2,3),\ \boldsymbol{\alpha}_2=\mathrm{diag}(4,3+\cos 3t,6),\ \boldsymbol{\alpha}_3=\mathrm{diag}(3,4,\cos t-5),\\ \boldsymbol{\beta}_1=\mathrm{diag}(2+\sin t,-3,1),\ \boldsymbol{\beta}_2=\mathrm{diag}(4,2,5+\cos t).\end{cases} \tag{32}$$

According to (21)-(32), the synchronization error in the numerical simulation is given as follows,

$$\boldsymbol{e}=\boldsymbol{\beta}_1\boldsymbol{y}_1+\boldsymbol{\beta}_2\boldsymbol{y}_2-\boldsymbol{\alpha}_1\boldsymbol{x}_1-\boldsymbol{\alpha}_2\boldsymbol{x}_2-\boldsymbol{\alpha}_3\boldsymbol{x}_3=\begin{pmatrix}e_1\\e_2\\e_3\end{pmatrix}=\begin{pmatrix}(2+\sin t)y_{11}+4y_{21}-(4+\sin t)x_{11}-4x_{21}-3x_{31}\\-3y_{12}+2y_{22}-2x_{12}-(3+\cos(3t))x_{22}-4x_{32}\\y_{13}+(5+\cos t)y_{23}-3x_{13}-6x_{23}-(\cos t-5)x_{33}\end{pmatrix}. \tag{33}$$

The initial values of all the system state variables and all the unknown parameters are selected as follows, $x_{11}=6$, $x_{12}=3$, $x_{13}=-4$, $x_{21}=2$, $x_{22}=-1$, $x_{23}=6$, $x_{31}=-2$, $x_{32}=5$, $x_{33}=-3$, $y_{11}=0$, $y_{12}=1$, $y_{13}=-2$, $y_{21}=-0.5$, $y_{22}=3$, $y_{23}=1$, $\tilde{a}_1=0.2$, $\tilde{a}_2=2$, $\tilde{a}_3=4$, $\tilde{b}_1=-0.1$, $\tilde{b}_2=0.2$, $\tilde{b}_3=-3$, $\tilde{c}_1=1$, $\tilde{c}_2=0.5$, $\tilde{c}_3=2$, $\tilde{d}_1=1$, $\tilde{d}_2=3$, $\tilde{d}_3=-1$, $\tilde{f}_1=4$, $\tilde{f}_2=6$, $\tilde{f}_3=3$.

According to the drive system group (21)-(23), the response system group (27)-(28), the scaling function matrices (32), the synchronization error (33), and the general formula of the adaptive controller (9), without loss of generality, we control the response system (28) and construct an adaptive controller as follows,

$$\begin{cases}u_1=\dfrac{1}{4}[-y_{11}\cos t-(2+\sin t)(y_{12}+y_{13})\tilde{d}_1-4(y_{22}-y_{21})\tilde{f}_1+x_{11}\cos t+(4+\sin t)(x_{12}-x_{11})\tilde{a}_1\\\qquad+4(x_{22}-x_{21})\tilde{b}_1+3(x_{32}-x_{31})\tilde{c}_1-\operatorname{sign}(e_1)|e_1|^{\alpha}-\operatorname{sign}(e_1)|e_1|^{\beta}],\\u_2=\dfrac{1}{2}[3y_{12}\tilde{d}_2-2y_{21}\tilde{f}_2+3y_{11}+2y_{21}y_{23}-3x_{22}\sin 3t+2x_{11}\tilde{a}_2+x_{22}\tilde{b}_2(3+\cos 3t)+4x_{32}\tilde{c}_2\\\qquad-2(x_{11}x_{13}+x_{12})-(7x_{21}+x_{21}x_{23})(3+\cos 3t)-4x_{31}x_{33}-\operatorname{sign}(e_2)|e_2|^{\alpha}-\operatorname{sign}(e_2)|e_2|^{\beta}],\\u_3=\dfrac{1}{5+\cos t}[y_{23}\sin t-y_{13}\tilde{d}_3+(5+\cos t)y_{23}\tilde{f}_3-(0.2+y_{11}y_{13})-4(5+\cos t)y_{21}^2-x_{33}\sin t+3x_{13}\tilde{a}_3\\\qquad-6x_{23}\tilde{b}_3-(\cos t-5)x_{33}\tilde{c}_3+3x_{11}x_{12}+6x_{21}x_{22}+(\cos t-5)x_{31}x_{32}-\operatorname{sign}(e_3)|e_3|^{\alpha}-\operatorname{sign}(e_3)|e_3|^{\beta}].\end{cases} \tag{34}$$

Based on (10), the identification laws of the drive system group (21)-(23) and the response system group (27)-(28) are written as follows,

$$\begin{cases}\dot{\tilde{a}}_1=-(4+\sin t)(x_{12}-x_{11})e_1+\operatorname{sign}(10-\tilde{a}_1)|10-\tilde{a}_1|^{\alpha}+\operatorname{sign}(10-\tilde{a}_1)|10-\tilde{a}_1|^{\beta},\\\dot{\tilde{a}}_2=-2x_{11}e_2+\operatorname{sign}(28-\tilde{a}_2)|28-\tilde{a}_2|^{\alpha}+\operatorname{sign}(28-\tilde{a}_2)|28-\tilde{a}_2|^{\beta},\\\dot{\tilde{a}}_3=-3x_{13}e_3+\operatorname{sign}(-8/3-\tilde{a}_3)|-8/3-\tilde{a}_3|^{\alpha}+\operatorname{sign}(-8/3-\tilde{a}_3)|-8/3-\tilde{a}_3|^{\beta}.\end{cases} \tag{35}$$

$$\begin{cases}\dot{\tilde{b}}_1=-4(x_{22}-x_{21})e_1+\operatorname{sign}(35-\tilde{b}_1)|35-\tilde{b}_1|^{\alpha}+\operatorname{sign}(35-\tilde{b}_1)|35-\tilde{b}_1|^{\beta},\\\dot{\tilde{b}}_2=-x_{22}e_2(3+\cos 3t)+\operatorname{sign}(28-\tilde{b}_2)|28-\tilde{b}_2|^{\alpha}+\operatorname{sign}(28-\tilde{b}_2)|28-\tilde{b}_2|^{\beta},\\\dot{\tilde{b}}_3=6x_{23}e_3+\operatorname{sign}(3-\tilde{b}_3)|3-\tilde{b}_3|^{\alpha}+\operatorname{sign}(3-\tilde{b}_3)|3-\tilde{b}_3|^{\beta}.\end{cases} \tag{36}$$

$$\begin{cases}\dot{\tilde{c}}_1=-3(x_{32}-x_{31})e_1+\operatorname{sign}(36-\tilde{c}_1)|36-\tilde{c}_1|^{\alpha}+\operatorname{sign}(36-\tilde{c}_1)|36-\tilde{c}_1|^{\beta},\\\dot{\tilde{c}}_2=-4x_{32}e_2+\operatorname{sign}(20-\tilde{c}_2)|20-\tilde{c}_2|^{\alpha}+\operatorname{sign}(20-\tilde{c}_2)|20-\tilde{c}_2|^{\beta},\\\dot{\tilde{c}}_3=(\cos t-5)x_{33}e_3+\operatorname{sign}(3-\tilde{c}_3)|3-\tilde{c}_3|^{\alpha}+\operatorname{sign}(3-\tilde{c}_3)|3-\tilde{c}_3|^{\beta}.\end{cases} \tag{37}$$

$$\begin{cases}\dot{\tilde{d}}_1=(2+\sin t)(y_{12}+y_{13})e_1-3y_{12}e_2+\operatorname{sign}(-1-\tilde{d}_1)|-1-\tilde{d}_1|^{\alpha}+\operatorname{sign}(-1-\tilde{d}_1)|-1-\tilde{d}_1|^{\beta},\\\dot{\tilde{d}}_2=-3y_{12}e_2+\operatorname{sign}(0.2-\tilde{d}_2)|0.2-\tilde{d}_2|^{\alpha}+\operatorname{sign}(0.2-\tilde{d}_2)|0.2-\tilde{d}_2|^{\beta},\\\dot{\tilde{d}}_3=y_{13}e_3+\operatorname{sign}(-5-\tilde{d}_3)|-5-\tilde{d}_3|^{\alpha}+\operatorname{sign}(-5-\tilde{d}_3)|-5-\tilde{d}_3|^{\beta}.\end{cases} \tag{38}$$

$$\begin{cases}\dot{\tilde{f}}_1=4(y_{22}-y_{21})e_1+\operatorname{sign}(10-\tilde{f}_1)|10-\tilde{f}_1|^{\alpha}+\operatorname{sign}(10-\tilde{f}_1)|10-\tilde{f}_1|^{\beta},\\\dot{\tilde{f}}_2=2y_{21}e_2+\operatorname{sign}(40-\tilde{f}_2)|40-\tilde{f}_2|^{\alpha}+\operatorname{sign}(40-\tilde{f}_2)|40-\tilde{f}_2|^{\beta},\\\dot{\tilde{f}}_3=-(5+\cos t)y_{23}e_3+\operatorname{sign}(2.5-\tilde{f}_3)|2.5-\tilde{f}_3|^{\alpha}+\operatorname{sign}(2.5-\tilde{f}_3)|2.5-\tilde{f}_3|^{\beta}.\end{cases} \tag{39}$$

Figure 1 shows the error curves of e_1, e_2 and e_3 respectively. The three synchronization errors not only tend to zero, but also the synchronization time is shorter than 3.928 423 s. All of these illustrate the controller given in Theorem 1 is effective. The fixed-time function combination synchronization of the drive system group and the response system group can be realized under the action of the controller.

The identification curves of the drive systems (21)-(23) and the response systems (27)-(28) are presented in Fig. 2 and Fig. 3.

Figure 2 shows the identification curves of the unknown parameters in the drive systems (21), (22) and (23) respectively. From Fig. 2, we can see the estimators of all the unknown parameters converge to their true values $a_1=10$, $a_2=28$, $a_3=-8/3$, $b_1=35$, $b_2=28$, $b_3=3$, $c_1=36$, $c_2=20$, $c_3=3$.

From Fig. 3, we can find that the estimators of all the unknown parameters in the response systems (27) and (28) converge to their true values $d_1=-1$, $d_2=0.2$, $d_3=-5$, $f_1=10$, $f_2=40$, $f_3=2.5$.

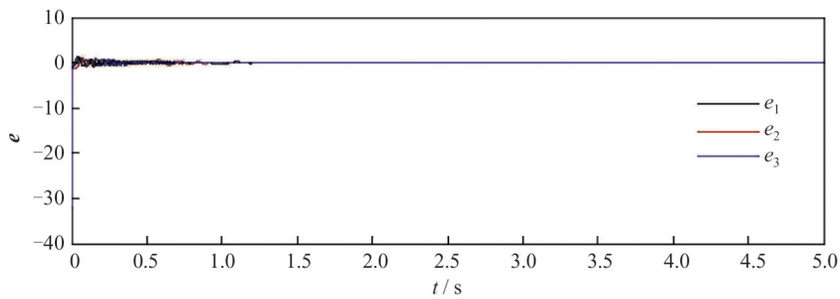


Fig. 1 The error trajectories of the drive system group (21)-(23) and the response system group (27)-(28)

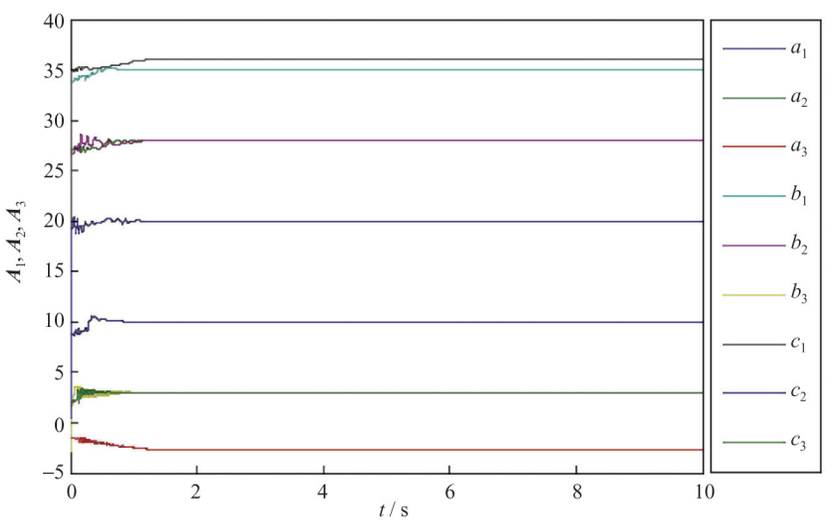


Fig. 2 The identification curves of the unknown parameters in drive systems (21)-(23)

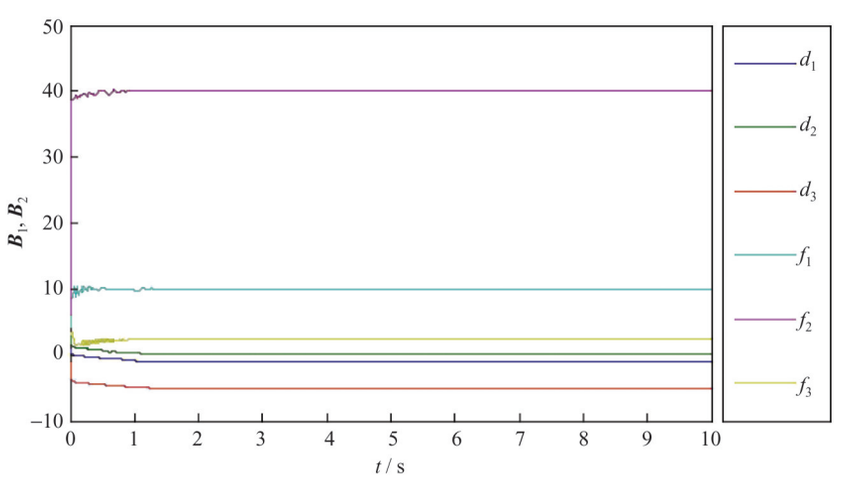


Fig. 3 The identification curves of the unknown parameters in the response system group (27)-(28)

We find that identification law (10) can accurately identify all the uncertain parameters of the drive system group and the response system group; all of these illustrate that the identification law is correct. The correctness of Theorem 1 is fully verified by the simulation results shown in Fig. 1, Fig. 2 and Fig. 3. Figure 4 and Fig. 5 show the time series of the two system groups and their function combinations, respectively.

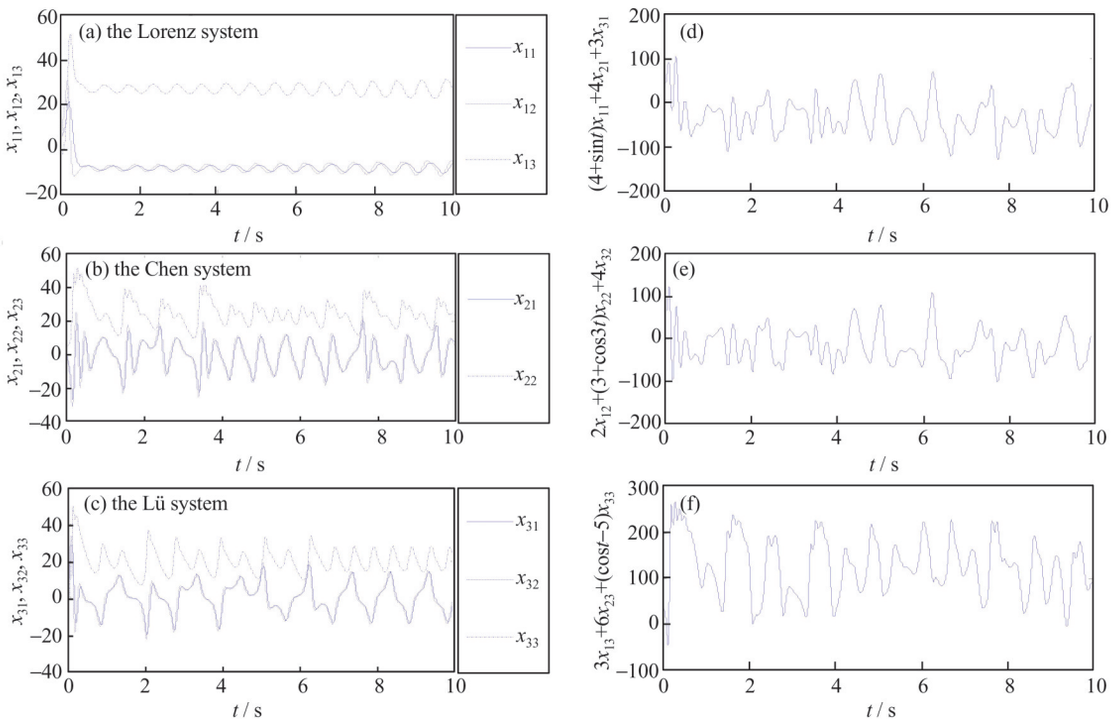


Fig. 4 The time series of three drive systems and their combination system

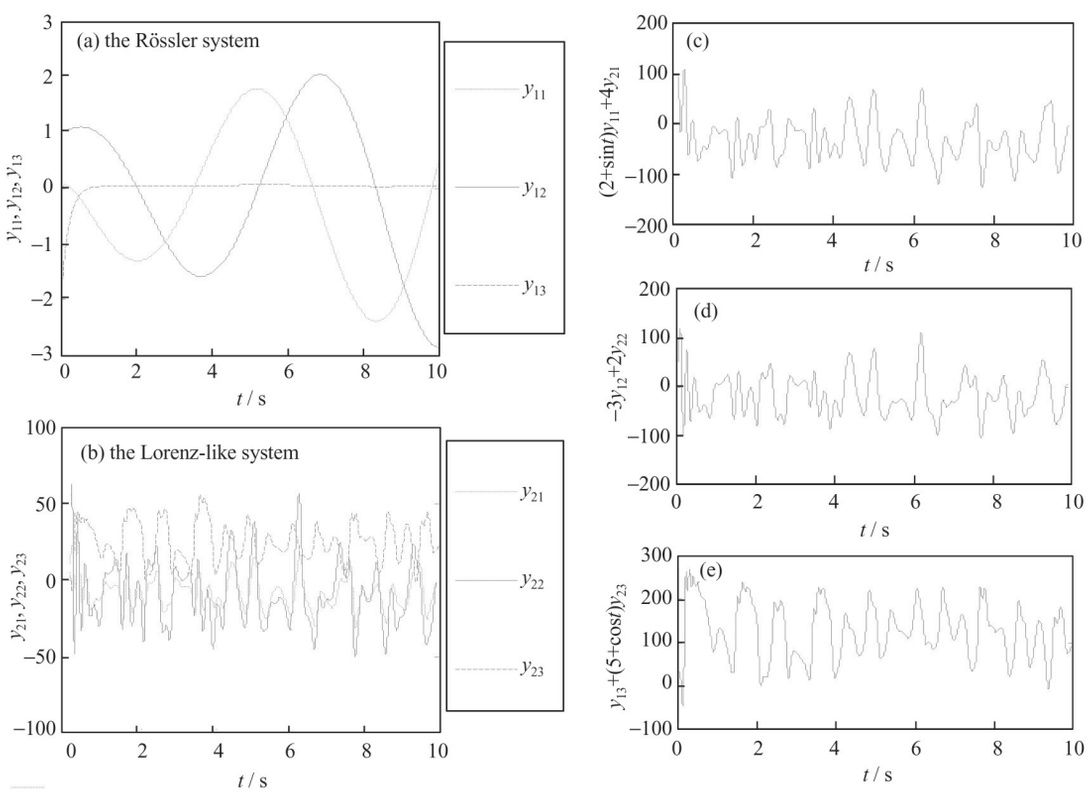


Fig. 5 The time series of two response systems and their combination system

To demonstrate the complexity of the function combination synchronization between the drive system group and the response system group, some time-series diagrams are given as follows.

Figure 4(a)-(c) show the time series of the three drive systems: (a), (b) and (c) correspond to the Lorenz, Chen and Lü chaotic systems, respectively. Figure 4(d)-(f) shows the time series of the function combination of the three drive systems. It is easy to find that the time series of the combination system are more complex than those of any single drive system: they are aperiodic and have larger amplitudes.

Figure 5(a) and (b) show the time series of the two response systems: (a) the Rössler system, which exhibits periodic behavior under the chosen parameter values, and (b) the Lorenz-like chaotic system. Figure 5(c)-(e) show the time series of the function combination of the two response systems. Similarly, the time series of the combination system are more complex than those of any single response system: they are aperiodic and have larger amplitudes. The error trajectories shown in Fig. 1 are obtained by subtracting the time series in Fig. 5(c)-(e) from those in Fig. 4(d)-(f), respectively.

5 Conclusion

Function combination synchronization of the drive system group and the response system group with unknown parameters has been studied, where the drive system group can consist of n chaotic systems and the response system group can consist of m chaotic systems. This synchronization pattern can be regarded as the most complex one and, in terms of the number of chaotic systems involved, a generalization of all the existing combination synchronization schemes; its time series can make the transmitted information more secure in secure communication.

The synchronization of the two system groups can be achieved by constructing only one adaptive controller to control only one system in the response system group. The constructed parameter identification laws of the drive system group and the response system group can accurately identify all the unknown parameters. The synchronization time of the fixed-time function combination synchronization of the drive system group and the response system group is given in a quantitative form.

References

[1] Pecora L M, Carroll T L. Synchronization in chaotic systems [J]. *Physical Review Letters*, 1990, **64**(8): 821-824.

[2] Zhang C L, Li J M. Hybrid function projective synchronization of chaotic systems with uncertain time-varying parameters via Fourier series expansion[J]. *International Journal of Automation and Computing*, 2012, **9**(4): 388-394.

[3] Luo C, Wang X Y. Hybrid modified function projective synchronization of two different dimensional complex nonlinear systems with parameters identification[J]. *Journal of the Franklin Institute*, 2013, **350**(9): 2646-2663.

[4] Li D K. Finite-time and fixed-time hybrid function projection synchronization of chaotic systems with unknown parameters[J]. *Journal of Lanzhou University* (*Natural Sciences*), 2023, **59**(4): 512-523(Ch).

[5] Wang H, Ye J M, Miao Z H, *et al*. Robust finite-time chaos synchronization of time-delay chaotic systems and its application in secure communication[J]. *Transactions of the Institute of Measurement and Control*, 2018, **40**(4): 1177-1187.

[6] Zhang W L, Yang T. Finite-time synchronization of discontinuous network systems via two control schemes[J]. *Franklin Open*, 2024, **6**: 100068.

[7] Zhang L Z, Zhong J, Lu J Q. Intermittent control for finite-time synchronization of fractional-order complex networks [J]. *Neural Networks*, 2021, **144**: 11-20.

[8] Chen C, Li L X, Peng H P, *et al*. Fixed-time synchronization of inertial memristor-based neural networks with discrete delay[J]. *Neural Networks*, 2019, **109**: 81-89.

[9] Kong F C, Zhu Q X, Sakthivel R. Finite-time and fixed-time synchronization analysis of fuzzy Cohen-Grossberg neural networks with discontinuous activations and parameter uncertainties[J]. *European Journal of Control*, 2020, **56**: 179-190.

[10] Zhang X, Zhou W N, Karimi H R, *et al*. Finite- and fixed-time cluster synchronization of nonlinearly coupled delayed neural networks via pinning control[J]. *IEEE Transactions on Neural Networks and Learning Systems*, 2021, **32**(11): 5222-5231.

[11] Jiang J H, Jin X Z, Chi J, *et al*. Distributed adaptive fixed-time synchronization for disturbed complex networks[J]. *Chaos*, *Solitons* & *Fractals*, 2023, **173**: 113612.

[12] Dong Y, Chen J W, Cao J D. Fixed-time pinning synchronization for delayed complex networks under completely inter-

mittent control[J]. *Journal of the Franklin Institute*, 2022, **359**(14): 7708-7732.

[13] Wang Y B, Min F H, Huang G, *et al*. Finite-time modified combination synchronization of memristive FitzHugh-Nagumo circuit with unknown disturbances[J]. *Chinese Journal of Physics*, 2020, **67**: 590-601(Ch).

[14] Sun J W, Wang Y, Wang Y F, *et al*. Compound-combination synchronization of five chaotic systems via nonlinear control [J]. *Optik*, 2016, **127**(8): 4136-4143.

[15] Sun J W, Fang J, Wang Y F, *et al*. Function combination synchronization of three chaotic complex systems[J]. *Optik*, 2016, **127**(20): 9504-9516.

[16] Mahmoud G M, Ahmed M E, Abed-Elhameed T M. On fractional-order hyperchaotic complex systems and their generalized function projective combination synchronization[J]. *Optik*, 2017, **130**: 398-406.

[17] Xi H L, Li Y X, Huang X. Adaptive function projective combination synchronization of three different fractional-order chaotic systems[J]. *Optik*, 2015, **126**(24): 5346-5349.

[18] Zheng S. Multi-switching combination synchronization of three different chaotic systems via nonlinear control[J]. *Optik*, 2016, **127**(21): 10247-10258.

[19] Khan A, Khattar D, Prajapati N. Dual combination combination multi switching synchronization of eight chaotic systems [J]. *Chinese Journal of Physics*, 2017, **55**(4): 1209-1218(Ch).

[20] Xiong K L, Yu J, Hu C, *et al*. Synchronization in finite/fixed time of fully complex-valued dynamical networks via non-separation approach[J]. *Journal of the Franklin Institute*, 2020, **357**(1): 473-493.

[21] Chen H K. Synchronization of two different chaotic systems: A new system and each of the dynamical systems Lorenz, Chen and Lü[J]. *Chaos*, *Solitons* & *Fractals*, 2005, **25**(5): 1049-1056.

[22] Kharabian B, Mirinejad H. Synchronization of Rossler chaotic systems via hybrid adaptive backstepping/sliding mode control[J]. *Results in Control and Optimization*, 2021, **4**: 100020.

[23] Sprott J C. Some simple chaotic flows[J]. *Physical Review E*, 1994, **50**(2): R647-R650.

具有未知参数的两个混沌系统组的固定时间函数组合同步

李德奎, 魏兴民, 吴建军

甘肃中医药大学 公共卫生学院, 甘肃 兰州 730101

摘要: 本文提出并研究了具有未知参数的两个混沌系统组的固定时间函数组合同步, 其中一个系统组称为驱动系统组, 由 n 个不同的混沌系统组成, 另一个由 m 个不同的混沌系统组成的系统组称为响应系统组。根据李雅普诺夫稳定性定理和自适应控制技术, 设计一个自适应控制器, 实现两个系统组的同步。虽然响应系统组中有很多个响应系统, 但是只需控制其中任何一个响应系统, 就能实现两个系统组的这种同步。同时, 设计的参数辨识法则能够准确辨识所有的未知参数, 同步时间不依赖于系统的初值。给出的一些数值实例证明了所得结论的正确性。

关键词: 函数组合同步; 未知参数辨识; 自适应控制器; 固定时间同步

□